

Impermeability of the GIRK2 weaver channel to divalent cations

Ping Hou, Anke Di, Ping Huang, Charlotte B. Hansen and Deborah J. Nelson

Am J Physiol Cell Physiol 278:1038-1046, 2000.

You might find this additional information useful...

This article cites 21 articles, 9 of which you can access free at:

<http://ajpcell.physiology.org/cgi/content/full/278/5/C1038#BIBL>

This article has been cited by 1 other HighWire hosted article:

Voltage-Gated Calcium Channels Mediate Intracellular Calcium Increase in Weaver Dopaminergic Neurons During Stimulation of D2 and GABAB Receptors

E. Guatteo, C. P. Bengtson, G. Bernardi and N. B. Mercuri

J Neurophysiol, December 1, 2004; 92 (6): 3368-3374.

[Abstract] [Full Text] [PDF]

Medline items on this article's topics can be found at <http://highwire.stanford.edu/lists/artbytopic.dtl> on the following topics:

Biochemistry .. Channel Subunit
Physiology .. Dopaminergic Neurons
Physiology .. Purkinje Cells
Developmental Biology .. Mesencephalon
Veterinary Science .. Cerebellum
Chemistry .. Cations

Updated information and services including high-resolution figures, can be found at:

<http://ajpcell.physiology.org/cgi/content/full/278/5/C1038>

Additional material and information about *AJP - Cell Physiology* can be found at:

<http://www.the-aps.org/publications/ajpcell>

This information is current as of December 30, 2008 .

Impermeability of the GIRK2 *weaver* channel to divalent cations

PING HOU, ANKE DI, PING HUANG, CHARLOTTE B. HANSEN, AND DEBORAH J. NELSON
*Department of Neurobiology, Pharmacology, and Physiology,
The University of Chicago, Chicago, Illinois 60637*

Hou, Ping, Anke Di, Ping Huang, Charlotte B. Hansen, and Deborah J. Nelson. Impermeability of the GIRK2 *weaver* channel to divalent cations. *Am J Physiol Cell Physiol* 278: C1038–C1046, 2000.—A single amino acid mutation (G156S) in the putative pore-forming region of the G protein-sensitive, inwardly rectifying K⁺ channel subunit, GIRK2, renders the conductance constitutively active and nonselective for monovalent cations. The mutant channel subunit (GIRK2^{wv}) causes the pleiotropic *weaver* disease in mice, which is characterized by the selective vulnerability of cerebellar granule cells and Purkinje cells, as well as dopaminergic neurons in the mesencephalon, to cell death. It has been proposed that divalent cation permeability through constitutively active GIRK2^{wv} channels contributes to a rise in internal calcium in the GIRK2^{wv}-expressing neurons, eventually leading to cell death. We carried out comparative studies of recombinant GIRK2^{wv} channels expressed in *Xenopus* oocytes and COS-7 cells to determine the magnitude and relative permeability of the GIRK2^{wv} conductance to Ca²⁺. Data from these studies demonstrate that the properties of the expressed current differ in the two systems and that when recombinant GIRK2^{wv} is expressed in mammalian cells it is impermeable to Ca²⁺.

potassium channels; *weaver* mice; G proteins; *Xenopus* oocytes; voltage clamp

THE MURINE *WEAVER* DISEASE is caused by the mutation of a single amino acid (G156S) in the putative pore region of the inwardly rectifying K⁺ channel, GIRK2. Previous studies have shown that recombinant GIRK2^{wv} expressed heterologously in *Xenopus* oocytes and mammalian cells, as well as in cerebellar granule cells from *wv* mice, formed homomultimeric channels characterized by 1) G protein insensitivity, 2) cation nonselectivity, and 3) sensitivity to QX314, MK-801, and verapamil inhibition.

Indirect evidence from a number of studies supports the hypothesis that the mutant *weaver* channel might render neurons leaky to Ca²⁺, eventually resulting in cell death. A recent study demonstrated that intracellular Ca²⁺ was elevated in the primary cerebellar neuronal cultures from heterozygous (*wv*/+) animals relative to wild type (4). Silverman and colleagues (14) have reported an apparent permeability of GIRK2^{wv} chan-

nels to Ca²⁺ over wild-type GIRK channels when expressed in *Xenopus* oocytes. In the Silverman et al. study, the Ca²⁺ permeability of the channel was inferred from the activation of the endogenous Ca²⁺-activated Cl⁻ conductance, which was seen only in GIRK2^{wv}-expressing oocytes (14). In parallel studies of recombinant GIRK2^{wv} channels in oocytes, removal of Ca²⁺ from the incubation medium was shown to significantly enhance oocyte survival (18). Taken together, these observations suggested that GIRK2^{wv} channels are permeable to monovalent as well as divalent cations.

In this study, we directly tested whether homomeric GIRK2^{wv} channels are permeable to Ca²⁺ in both *Xenopus* oocytes and mammalian cells transiently expressing GIRK2^{wv} channels in culture. Homomeric channels were weakly permeable to Ca²⁺ in the *Xenopus* oocytes. In contrast, the divalent cation permeability was absent in the GIRK2^{wv}-expressing mammalian cells, suggesting that susceptibility to cell death in GIRK2^{wv}-expressing neurons may simply be due to Ca²⁺ influx through parallel, voltage-dependent channels following prolonged depolarization.

MATERIALS AND METHODS

cDNA clone. GIRK1 was cloned from a RIN cell library and had a predicted amino acid sequence identical to the cardiac clone originally described (8). GIRK2 and GIRK2^{wv} were gifts from Dr. P. Kofuji (California Institute of Technology, CA). The m2 muscarinic receptor was purchased from Clontech (Clontech, CA) in the pGEM3Z vector. All GIRK constructs were subcloned into either the pMXT vector, obtained from Dr. P. Kofuji, for oocyte expression or pEGFPN3 (Clontech, CA) for mammalian expression. The m2 receptor was linearized with *Hind* III, and cRNA was transcribed using the T7 polymerase mMessage mMachine kit (Ambion, Austin, TX). All GIRK constructs were linearized with *Sal* I, and cRNA was transcribed using T3 polymerase mMessage mMachine kit (Ambion). The cRNA concentration was determined by ultraviolet light absorption at 260 nm (A₂₆₀) and confirmed by intensity on ethidium bromide stained agarose gels. For mammalian cell expression, GIRK1, GIRK2, and GIRK2^{wv} were fused to enhanced green fluorescent protein (EGFP) at the carboxy terminus in the pEGFPN3 vector (Clontech).

Oocyte electrophysiology. Oocytes were injected with 2 ng of m2 muscarinic receptor cRNA and 5 ng of each GIRK subunit cRNA along with 12.3 ng GIRK5 (KHA1) antisense cRNA. Injected oocytes were maintained in OR-2+ solution containing (in mM) 96 NaCl, 2.5 KCl, 1 CaCl₂, 1 MgCl₂, 5 HEPES, 2.5 sodium pyruvate, and 50 µg/ml gentamicin. Nominally Ca²⁺-free solutions were used to incubate and maintain oocytes expressing GIRK2^{wv}.

The costs of publication of this article were defrayed in part by the payment of page charges. The article must therefore be hereby marked "advertisement" in accordance with 18 U.S.C. Section 1734 solely to indicate this fact.

Two-microelectrode voltage-clamp recordings were performed 3 days postinjection using a TURBO TEC-10C amplifier (NPI, Tamm, Germany). Data were acquired using Pulse software (HEKA, Lambrecht, Germany), an ITC-16 interface (Instrutech, Great Neck, NY), and an IBM-compatible PC. Microelectrodes were filled with 3 M KCl and had resistances of 0.5–2 MΩ. During electrophysiological recordings, oocytes were continuously superfused with a bath solution of 90 mM NaCl or KCl, 1 mM MgCl₂, and 5 mM HEPES (pH 7.6 with NaOH/KOH). Na⁺ was isosmotically replaced with *N*-methyl-D-glucamine (NMDG) in solutions used to investigate divalent permeability. The divalent content of these solutions was varied at constant osmolality and contained (in mM) 5, 20, or 70 CaCl₂ and 90, 70, or 20 NMDG-Cl, 1 MgCl₂, 5 HEPES (pH 7.6 with HCl). G protein-dependent currents were induced with the addition of 5 μM carbachol (Sigma, St. Louis, MO) to the bathing solution. In all experiments, the holding potential was –80 mV; test potentials were delivered once every second and stepped between –150 and 50 mV in 20-mV increments. Data collection and analysis were performed using Pulse/Pulse Fit (HEKA), and data plotted using the integrated graphics package IGOR (WaveMetrics, Lake Oswego, OR). Data are presented as means ± SE. The level of significance for the data in Figs. 5 and 6 was determined using ANOVA type analysis, General Linear Models, with the Tukey correction (SAS, Cary NC) for unequal cell sizes. All experiments were conducted at room temperature.

Mammalian cell culture and cDNA transfection. COS-7 cells (American Type Culture Collection) were plated in 35-mm dishes and grown in DMEM supplemented with 10% fetal bovine serum, 100 U/ml penicillin, and 100 μg/ml streptomycin. Transfection of COS-7 cells was carried out using SuperFect Transfection Reagent (10 μl per dish; QIAGEN, Valencia, CA) mixed with the following amounts of cDNA: 0.5 μg m2R with 1 μg GIRK1-EGFP and GIRK2 or GIRK2_{wv}-EGFP in 100 μl serum-free media (Opti-MEM1; GIBCO, Grand Island, NY). Cells were exposed to the DNA-containing solution for 10 min at room temperature, followed by the addition of 600 μl of serum-containing cell culture media. Cells were then incubated for 2 h, washed once, and incubated at 37°C, 5% CO₂. Electrophysiological recordings from COS-7 cells were made 48 h from transfection initiation on green fluorescent protein positive cells.

Electrophysiological recording from mammalian cells. Whole cell recordings were performed at room temperature 48–72 h posttransfection in an initial bath solution consisting of (in mM) 140 NaCl, 5.4 KCl, 2 CaCl₂, 1 MgCl₂, and 10 HEPES, pH 7.4. After currents in low-K⁺ solutions were recorded, cells were superfused with either a high-K⁺ solution containing (in mM) 140 KCl, 1 MgCl₂, and 10 HEPES, pH 7.4, or a high-Na⁺ solution containing (in mM) 145 NaCl, 1 MgCl₂, and 10 HEPES, pH 7.4. In experiments designed to quantitate the Ca²⁺ permeability, cells were superfused with 5 or 70 mM Ca²⁺ bath solution containing (in mM) 5 CaCl₂ with 140 NMDG-Cl, or 70 CaCl₂ with 35 NMDG-Cl, 1 MgCl₂, 10 HEPES, pH 7.4. Solution osmolality was kept constant at 270–290 mosM using a vapor pressure osmometer (Wescor, Logan, UT). Patch pipettes were pulled from microhematocrit capillary tubes (Fisherbrand, Fisher, Pittsburgh, PA) to give resistances of 3–6 MΩ. The pipette recording solution contained (in mM) 120 KCl, 2 CaCl₂, 1 MgCl₂, 11 EGTA, 33 KOH, 10 HEPES, 1 NaGTP, 2 MgATP, pH 7.2, or 140 NMDG, 0.2 CaCl₂, 1 MgCl₂, 1 EGTA, 10 HEPES, 1 NaGTP, 2 MgATP, pH 7.2 when Ca²⁺ currents were measured. Whole cell currents were recorded with an EPC-7 (List Electronics, Lambrecht, Germany) patch-clamp amplifier at 2 kHz and low-pass filtered at 1 kHz. Stimulation and data acquisition were controlled by the

PULSE software package on a Power Macintosh computer, and data analysis was performed with IGOR software (WaveMetrics, Lake Oswego, OR).

Digital fluorescent imaging. COS-7 cells were grown on 25-mm coverslips to 50% confluence, loaded with 2 μM fura 2-AM (Molecular Probes) in serum-free MEM for 1 h, then equilibrated in Hanks' balanced saline solution (HBSS; GIBCO, Grand Island, NY) for 50 min. Fura 2 loading and equilibration were carried out at 37°C. The coverslip with loaded cells was moved into a Teflon coverslip recording dish (model LU-CSD; Medical Systems, NY) and mounted on the microscope stage. Cells were continuously superfused throughout the experiment with HBSS or switched to a 70 mM Ca²⁺ solution containing (in mM) 70 CaCl₂ with 35 NMDG-Cl, 1 MgCl₂, and 10 HEPES, pH 7.4. Internal Ca²⁺ (Ca_i) was determined using digital fluorescent imaging of cellular fura 2 epifluorescence. Emission was determined at 510 nm following excitation at 340 and 380 nm. Images were obtained every 20 s, and 64 frames were averaged at each excitation wavelength. Background was obtained using an area of the coverslip devoid of cells and subtracted from each excitation wavelength image. After background subtraction, the 340-nm image was divided by the 380-nm image to provide a ratio (R) image. Image analysis was carried out using the ImageMaster Ratio Fluorescence Imaging Software (Photon Technology International, NJ).

RESULTS

Comparison of GIRK1/2 and GIRK2_{wv} channels expressed in *Xenopus* oocytes and COS-7 cells. The goal of this study was to quantitate the magnitude of the Ca²⁺ permeability of recombinant GIRK2_{wv} channels compared with heteromultimeric GIRK1 + GIRK2 (GIRK1/2) channels. We compared expression of the wild-type and mutant channels in *Xenopus* oocytes to that in mammalian COS-7 cells.

Recombinant GIRK subunits coassemble with endogenous *Xenopus* GIRK5 subunits to form functional channels (5). Antisense cRNA against GIRK5 (KHA1) has been previously reported to knock out endogenous GIRK5 expression in oocytes (5, 15). Therefore, antisense cRNA against GIRK5 was coinjected in all our studies to prevent endogenous GIRK5 expression and coassembly.

Figure 1, *A* and *B*, compares expression of the heteromultimeric GIRK1/2 conductance in a representative *Xenopus* oocyte and mammalian cell. Both expression systems gave rise to carbachol-induced currents that were inwardly rectifying and Ba²⁺ sensitive. When expressed in oocytes, GIRK1/2 was associated with a large basal (carbachol-independent) current in high-K⁺ solutions. The corresponding basal current was absent in the COS-7 cells. Average peak current amplitude of the carbachol-sensitive K⁺ current was $-3.5 \pm 0.3 \mu\text{A}$ ($n = 41$) at -150 mV in *Xenopus* oocytes and $-1.2 \pm 0.3 \text{ nA}$ at -160 mV ($n = 5$) in COS-7 cells.

As has been previously observed in a number of other laboratories, the *weaver* mutation in GIRK2 induces the expression of recombinant channels, which are highly permeable to Na⁺ and independent of G protein-induced gating, as can be seen in Fig. 2, *A* and *B*. Large basal currents in both high-Na⁺ and high-K⁺ solutions were observed in oocytes as well as COS-7 cells. The magnitude of the G protein-independent Na⁺ current

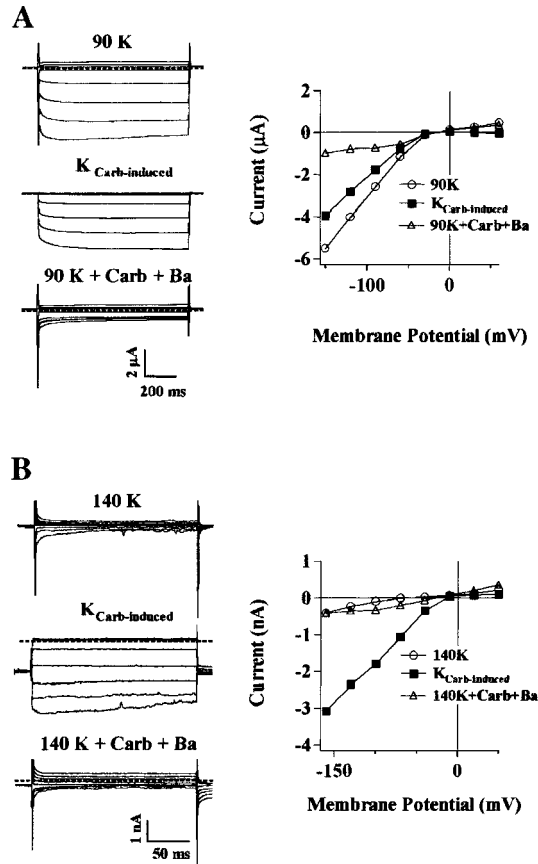


Fig. 1. Coexpression of GIRK1 with GIRK2 in *Xenopus* oocytes leads to larger G protein-independent currents than coexpression in mammalian cells. **A**: 2 microelectrode current recordings from an oocyte injected with cRNA for m2 muscarinic receptors, GIRK1 and GIRK2. **A, left**: 3 families of superimposed current traces elicited by 1-s voltage steps to potentials between -150 and 50 mV from a holding potential of -80 mV. Dotted lines, zero current level. First set of currents was recorded from an oocyte in a solution in which all the NaCl was replaced with KCl. Second set of currents represents carbachol (Carb)-induced currents obtained by subtracting currents recorded in high-K⁺ solution from those recorded in a high K⁺ solution containing in addition $5 \mu\text{M}$ carbachol. Third set of currents represents residual current remaining after adding $500 \mu\text{M}$ Ba²⁺ to high-K⁺ carbachol-containing solution. All 3 families of current were obtained from the same oocyte. Corresponding current-voltage (*I-V*) relations are plotted to *right* of current traces. Current magnitude was determined at the point in the current traces where the currents were maximum. **B**: whole cell patch voltage-clamp recordings from a single COS-7 cell transiently transfected with the GIRK1-EGFP and GIRK2 cDNA along with m2 receptor cDNA as described in MATERIALS AND METHODS. Cells chosen for electrophysiological recording were identified by their green fluorescence. **B, left**: 3 families of superimposed current traces elicited by 200-ms voltage steps to potentials between -160 and 50 mV from a holding potential of -80 mV. As in **A**, the dotted lines indicate zero current level. First set of currents was recorded in a solution in which all the external NaCl was isosmotically replaced with KCl. Second set of currents represents difference currents obtained by subtracting currents in high-K⁺ solution from those obtained in the identical solution containing in addition $5 \mu\text{M}$ carbachol. Third set of current traces was obtained when $200 \mu\text{M}$ Ba²⁺ was added to high-K⁺ carbachol-containing solution. Associated *I-V* relationships are plotted to *right* of current traces. Note that, compared with the current GIRK1/2 currents recorded in the oocyte in high-K⁺ solutions, currents recorded from the mammalian cell preparations failed to show a significant expression of G protein-independent (basal) current activation.

at -150 mV was $-3.3 \pm 0.4 \mu\text{A}$ ($n = 30$) in oocytes and $-1.3 \pm 0.2 \text{ nA}$ ($n = 4$) in the COS-7 cells. External solutions in the oocyte experiments were nominally Ca²⁺ free to prevent activation of the endogenous Ca²⁺-activated Cl⁻ current due to influx of Ca²⁺ through either the GIRK2_{wv} channel itself or through endogenous, depolarization-activated Ca²⁺-permeable pathways. Note that the currents expressed in the *Xenopus* oocytes failed to show the pronounced inward rectification as observed for GIRK2_{wv} expression in the COS-7 cells. The relative absence of inward rectification in both K⁺- and Na⁺-containing solutions was consistent for all oocytes expressing GIRK2_{wv}.

The cation channel blocker QX-314 has been reported to be an effective inhibitor of GIRK2_{wv} currents in oocytes expressing GIRK2_{wv} channels with an IC₅₀ of $10.5 \mu\text{M}$ in high-K⁺ external solutions (6). Figure 2 compares the relative efficacy of QX-314-induced inhibition of monovalent current through GIRK2_{wv} channels in oocytes vs. COS-7 cells. QX-314 ($300 \mu\text{M}$) produced a $70 \pm 12\%$ ($n = 5$) decrease in current amplitude at -160 mV in high-Na⁺ solutions in COS-7 cells. The QX-314-induced inhibition of GIRK2_{wv} currents ex-

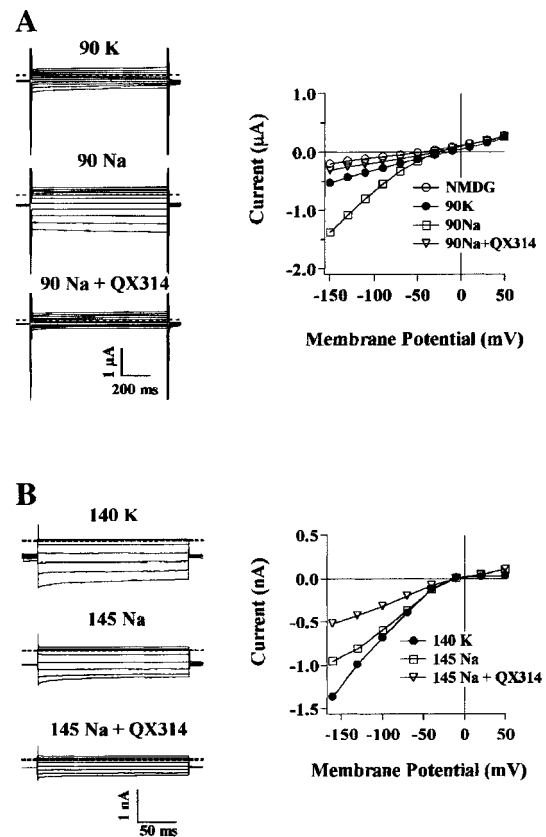


Fig. 2. Comparison of GIRK2_{wv} expression in *Xenopus* oocytes and mammalian cells. **A**: currents were recorded from oocytes as in Fig. 1A. Three families of current traces shown at *left* were recorded in solutions containing high K⁺, high Na⁺, high Na⁺ containing $300 \mu\text{M}$ QX314, and a solution in which all the monovalent cations had been replaced with *N*-methyl-D-glucamine (NMDG). Associated *I-V* relations are plotted to the *right*. **B**: currents recorded from a single transfected mammalian cell as in Fig. 1B. External solutions are given above each family of current traces. Associated *I-V* relationships are plotted to the *right*.

pressed in the oocytes was $74 \pm 4\%$ ($n = 5$) at -150 mV also in high-Na⁺ external solutions. The percentage of QX-314-induced current inhibition in the oocytes was calculated following leak subtraction. Leak current was determined in solutions in which all the permeant cations were isosmotically replaced with the large impermeant cation NMDG. It should be noted that QX-314 failed to inhibit monovalent cation current in a small percentage of oocytes in which the leak-subtracted GIRK2_{wv} current-voltage (*I-V*) relationship was linear (data not shown).

Divalent permeability of uninjected oocytes. To quantify the magnitude of the GIRK2_{wv}-induced Ca²⁺ influx pathway, it was necessary to identify basal divalent permeability through endogenous, voltage-gated Ca²⁺ channels in uninjected oocytes exposed to solutions containing elevated divalent concentrations. Characterization of endogenous voltage-activated Ca²⁺ channels in oocytes has been previously established (2, 9, 12). A comparative summary of the magnitude of both inward and outward current at -150 and 50 mV, in high and low Ca²⁺ solutions is plotted in Fig. 3 as a function of internal 1,2-bis(2-aminophenoxy)ethane-*N,N,N',N'*-tetraacetic acid (BAPTA) buffering. Charney and colleagues (1) have previously reported the use of BAPTA injections to buffer the influx of Ca²⁺ in oocytes, thereby preventing activation of the endogenous Ca²⁺-activated anion conductance.

As can be seen in Fig. 3A, oocytes exposed to extracellular solutions containing 70 mM Ca²⁺ showed significant outward current at 50 mV [$2,400 \pm 380$ nA ($n = 8$)] compared with currents in 5 mM Ca²⁺-containing solutions [450 ± 57 nA ($n = 8$)]. The enhancement of outward current in high Ca²⁺ at the depolarized potential was prevented if the oocytes were injected with 50 nl of 100 mM BAPTA before current recording. Inward currents showed no significant change in amplitude on

raising external Ca²⁺ and were unaffected by internal BAPTA buffering. Outward currents at 50 mV in the presence of internal BAPTA buffering were 330 ± 28 and 250 ± 26 nA ($n = 6$) in 5 and 70 mM Ca²⁺, respectively (Fig. 3B). A relative comparison of current amplitude at -150 and 50 mV for the high- and low-Ca²⁺-containing solutions in the presence and absence of internal BAPTA buffering is given in Fig. 3C.

Direct measurement of current carried by Ca²⁺ in oocytes and mammalian cells expressing GIRK1/2 and GIRK2_{wv}. To determine the magnitude of divalent current carried by GIRK2_{wv} channels compared with GIRK1/2 channels, experiments on both oocytes and COS-7 cells were performed in solutions in which Ca²⁺ was the only permeant cation in the extracellular solution. Oocytes were injected with 100 mM BAPTA prior to current recording in high divalent solutions to block activation of the contaminating Ca²⁺-activated Cl⁻ current. Figure 4 illustrates data obtained from both oocytes and COS-7 cells expressing GIRK1/2. Both basal and carbachol-induced K⁺ currents were recorded to ensure that cells were expressing G protein-activated GIRK channels. Sequential exposure of COS-7 cells to 5 and 70 mM Ca²⁺-containing solutions failed to result in current activation. Current amplitudes at -150 mV for oocytes showed no significant change on switching from low to high external Ca²⁺.

A comparison of current data obtained from both oocytes and COS-7 cells expressing either GIRK1/2 or GIRK2_{wv} channels in external solutions containing 5 mM Ca²⁺ is given in Fig. 5, A and B. Current in solutions containing high Na⁺ was recorded to confirm that cells were expressing GIRK2_{wv} channels. Exposure of COS-7 cells to 5 mM Ca²⁺-containing solutions did not elicit current activation. However, Ca²⁺ currents were observed in 5 mM Ca²⁺ solutions in oocytes expressing GIRK2_{wv} channels. A comparison of cur-

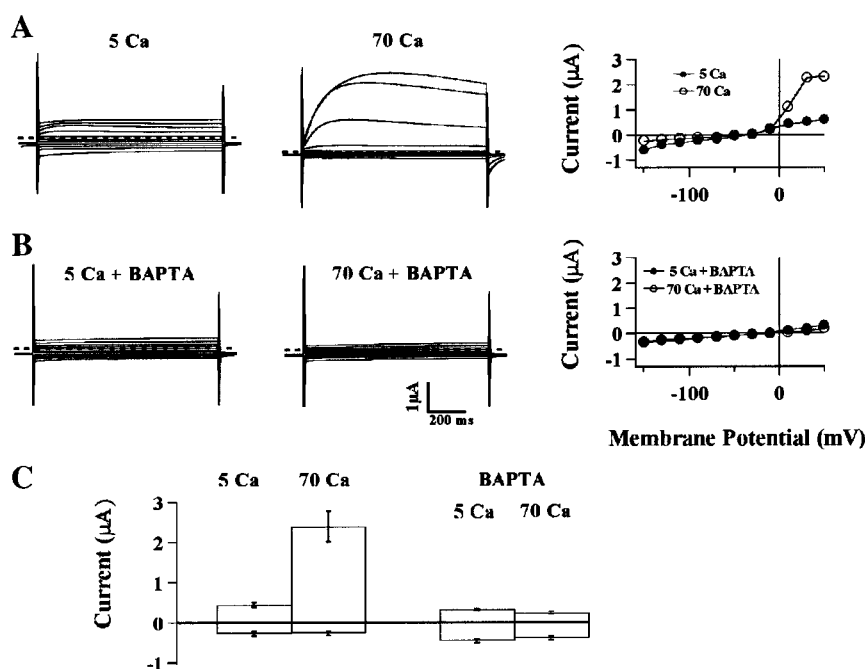


Fig. 3. Summary of inward and outward current amplitudes in uninjected oocytes as a function of increasing external divalent concentrations in the presence and absence of internal BAPTA buffering. All experiments were obtained from uninjected oocytes using voltage protocols described in Fig. 1. Oocytes were injected with high concentrations of BAPTA as described in MATERIALS AND METHODS. A: representative currents and *I-V* relationship from a single oocyte in solutions containing 5 and 70 mM Ca²⁺ as the only permeant species. B: currents from an oocyte injected with BAPTA in the presence of the low and high Ca²⁺-containing solutions. C: comparison of current amplitude for two Ca²⁺-containing solutions in the presence and absence of internal Ca²⁺ buffering. Peak current amplitude was determined at 50 and -150 mV. In all experiments, Ca²⁺ was the only permeant cation in the external solution. Isosmolarity was obtained by addition of sucrose to the low-Ca²⁺ solution.

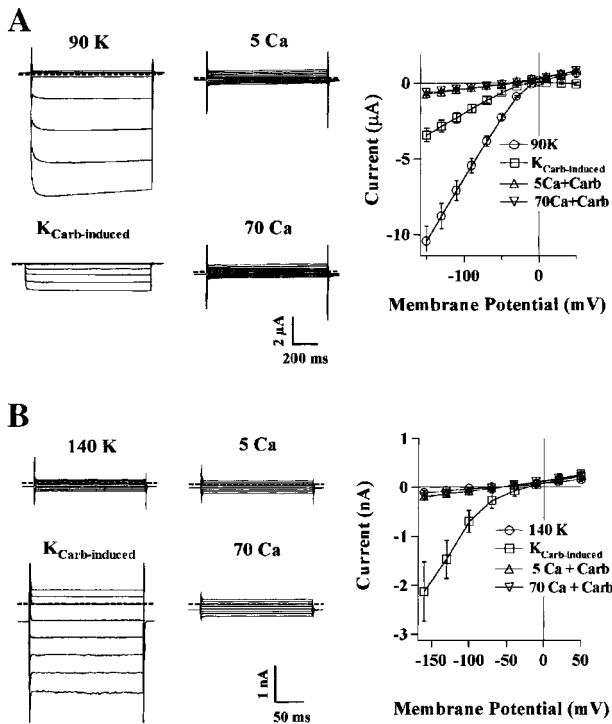


Fig. 4. Elevation in extracellular Ca^{2+} fails to result in an increase in inward current or change in reversal potential in GIRK1/2-expressing oocytes as well as mammalian cells. *A*: 2 microelectrode voltage-clamp experiments were carried out on GIRK1/2-expressing oocytes as in Fig. 1*A*. *Left*: G protein independent currents and carbachol-induced currents in high- K^+ solutions and currents obtained in solutions in which Ca^{2+} was the only permeant species. Average *I-V* relationships are given to the *right* of the current traces for 7 cells in which similar experiments were carried out. Note that there was no significant increase in current in changing from a low to high Ca^{2+} -containing solution as seen in the average *I-V* relationship. *B*: identical experiments carried out in transiently transfected COS-7 cells. Average *I-V* relationships were obtained in a total of 5 cells. Note the absence of a G protein independent current or current increases on exchanging to extracellular solutions containing high Ca^{2+} .

rents recorded in 70 mM Ca^{2+} -containing solutions from representative oocytes and COS-7 cells expressing GIRK1/2 and GIRK2_{wv} channels is shown in Fig. 6. There was a statistically significant increase in GIRK2_{wv} Ca^{2+} current over that observed for GIRK1/2 in the oocyte expression studies (Fig. 6*A*). Inward current for GIRK2_{wv}-expressing oocytes was 910 ± 97 nA ($n = 15$) in 5 mM Ca^{2+} and $1,175 \pm 190$ nA ($n = 5$) in 70 mM Ca^{2+} . This is to be compared with a current amplitude of 628 ± 72 nA ($n = 8$) and 568 ± 52 nA ($n = 8$) for GIRK1/2-expressing oocytes in 5 and 70 mM Ca^{2+} , respectively. There was a positive 12-mV potential shift in the reversal potential on increasing the external divalent concentration in oocytes expressing GIRK2_{wv}. The reversal potential was -13.5 ± 1.3 mV ($n = 15$) for 5 mM Ca^{2+} and -1.3 ± 3.6 mV ($n = 5$) for 70 mM Ca^{2+} . We also examined divalent currents in oocytes expressing GIRK2_{wv} in 20 mM Ca^{2+} . Current amplitude in these experiments [$1,029 \pm 136$ nA ($n = 10$)] was not significantly different from that in 70 mM Ca^{2+} [$1,175 \pm 190$ nA, ($n = 5$)]. The reversal potential in control (uninjected) oocytes was -34 ± 2.6 mV ($n = 5$) and -32.7 ± 3 mV ($n = 5$) in 5 and 70 mM Ca^{2+} -

containing solutions, demonstrating that the shifts in reversal potential in the GIRK2_{wv}-expressing oocytes were not attributable to a background current. Ca^{2+} current in the GIRK2_{wv}-expressing oocytes in the presence of QX314 was $1,032 \pm 277$ nA ($n = 7$) in 20 mM Ca^{2+} and did not change from current recorded in the absence of QX314, indicating that either the GIRK2_{wv} channel when expressed in oocytes is not sensitive to QX314 in the presence of high external divalent concentrations or that the divalent permeable pathway is not due to GIRK2_{wv} expression. Niflumic acid, a potent Ca^{2+} -activated Cl^- channel blocker in oocytes with a dissociation constant (K_d) of 17 μM (20) did not inhibit outward or inward current at a concentration of 1 mM (data not shown), indicating that the QX314-insensitive divalent current was not due to the endogenous Ca^{2+} -activated Cl^- channels.

We were unable to observe either an increase in current or shift in reversal potential on increasing external Ca^{2+} in COS-7 cells expressing GIRK2_{wv} channels. The reversal potential in the mammalian cell experiments was -28.6 ± 5.2 mV ($n = 5$) in 5 mM Ca^{2+} and -23.0 ± 5.6 mV ($n = 5$) in 70 mM Ca^{2+} -containing solutions.

Intracellular calcium measurements. To further investigate whether constitutively active GIRK2_{wv} channels expressed in mammalian cells could give rise to significant changes in levels of intracellular calcium (Ca_i), as has been reported for neurons cultured from *weaver* mice (4, 21), we carried out digital fluorescent imaging experiments in COS-7 cells transfected with GIRK1/2 or GIRK2_{wv} where GIRK1 and GIRK2_{wv} were tagged with EGFP. Fura 2 was used to detect resting Ca_i in nontransfected COS-7 cells, COS-7 cells cotransfected with GIRK1-EGFP, and GIRK2 or COS-7 cells transfected with GIRK2_{wv}-EGFP. Cells were loaded with fura 2-AM for 1 h before digital fluorescent imaging experiments. The resting 340/380 ratios (R) among the three groups were indistinguishable. These data are summarized in Fig. 7. The dynamic range of the cellular response to changes in Ca_i was determined in experiments in which cells were sequentially exposed to a solution containing 10 μM ionomycin in the presence of 2 mM Ca^{2+} , followed by a solution change to one in which the free Ca^{2+} concentration was buffered to zero in the presence of 1 mM EGTA as seen in Fig. 7*A*. The mean resting 340/380 nm fluorescence intensity ratio ($R_{340/380}$) values were 0.6 ± 0.02 ($n = 43$) for nontransfected cells, 0.55 ± 0.09 ($n = 32$) for GIRK1/GIRK2-expressing cells, and 0.57 ± 0.03 ($n = 34$) for the GIRK2_{wv}-expressing cells (Fig. 7*B*). We were unable to detect a change in the $R_{340/380}$ values on changing from low (2 mM) to high (70 mM) external Ca^{2+} in either the GIRK1/2- or GIRK2_{wv}-transfected cells. The average of the change in the $R_{340/380}$ in individual cells on increasing extracellular Ca^{2+} from 2 to 70 mM was 0.28 ± 0.02 ($n = 5$) for GIRK1/2 and 0.21 ± 0.03 ($n = 9$) for GIRK2_{wv} as summarized in Fig. 7*C*.

DISCUSSION

Expression and activation of GIRK2_{wv} in oocytes has been associated with a large increase in the endogenous

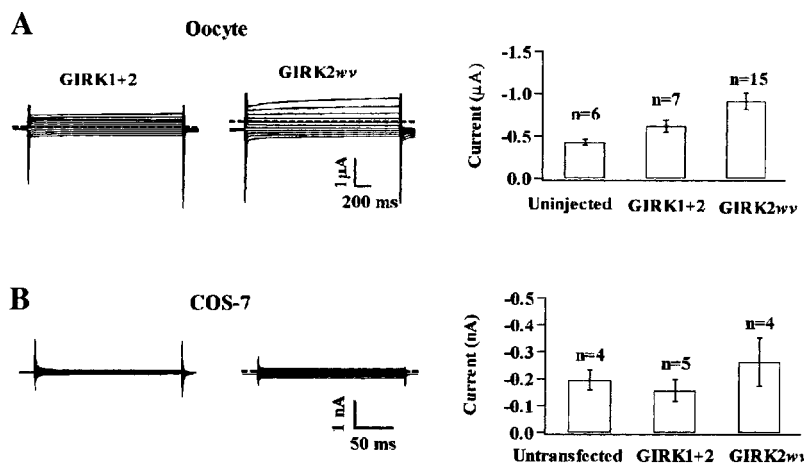


Fig. 5. GIRK2_{wv} expression in oocytes but not mammalian cells gives rise to a significant inward current in 5 mM Ca²⁺-containing solutions over that seen in GIRK1/2-expressing cells. *A*: experiments were carried out in divalent solutions using voltage protocols as in Fig. 1. Current traces are from representative oocytes expressing GIRK1/2 and GIRK2_{wv}. Amplitude of the inward current at -150 mV for uninjected, GIRK1/2, and GIRK2_{wv}-expressing oocytes is compared on *right*. Divalent inward current was significantly greater in the GIRK2_{wv}-expressing oocytes over that observed for the GIRK1/2-expressing oocytes ($P < 0.001$) as well as for the uninjected oocytes ($P < 0.0001$). Level of significance between mean currents in 3 populations of oocytes was determined using General Linear Models (SAS, Carey, NC) with a Tukey correction for analysis of unequal cell sizes. *B*: currents from representative COS-7 cells transiently transfected with GIRK1-EGFP + GIRK2 and GIRK2_{wv}-EGFP fusion protein. There was no significant increase in inward current in 2 mM Ca²⁺-containing solutions for the GIRK2_{wv} cells over that seen for the GIRK1/2-expressing cells as summarized in the bar graph to the *right* of the current traces.

Ca²⁺-activated Cl⁻ current, indicative of a large divalent influx in Ca²⁺-containing solutions (14). This observation, along with the increased vulnerability of oocytes to cell death in Ca²⁺-containing solutions (18), has suggested that the GIRK2_{wv} channel might allow for a significant Ca²⁺ “leak.” These observations prompted our investigation of the magnitude of the GIRK2_{wv}

divalent permeability in heterologous expression systems.

In this study, we have compared expression of GIRK1/2 and GIRK2_{wv} channels in both oocytes and mammalian cells. We compared the divalent permeability of the wild-type to the mutant GIRK2_{wv} channels and found that oocytes expressing the mutant channels

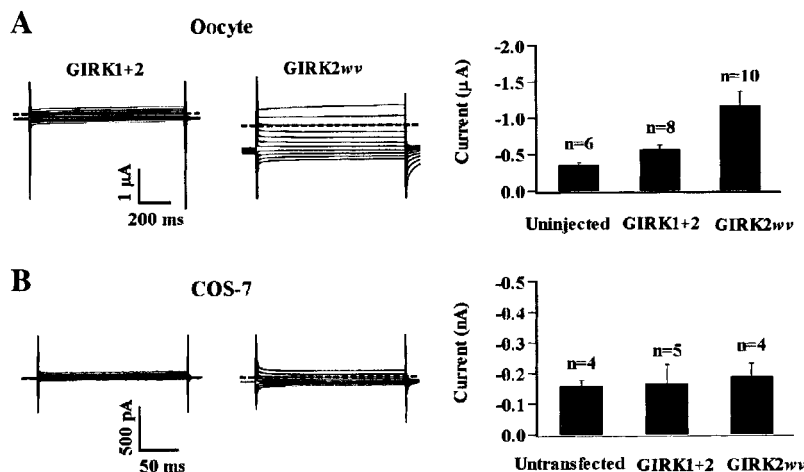


Fig. 6. Comparison of representative currents recorded from oocytes and mammalian cells expressing GIRK1/2 and GIRK2_{wv} in 70 mM Ca²⁺-containing solutions. *A*: representative families of current traces from 2 different oocytes expressing either GIRK1+2 or GIRK2_{wv} in external solutions containing 70 mM external Ca²⁺. Summary of maximum inward current at -150 mV is given to *right* of the current traces. Inward current in the GIRK2_{wv}-expressing oocytes was significantly increased ($P < 0.001$) over that observed for the GIRK1/2-expressing oocytes. Statistical analysis was performed as in Fig. 5, comparing mean inward current data between uninjected, GIRK1 + GIRK2, and GIRK2_{wv}-expressing oocytes. Results of statistical analysis demonstrated that in the oocytes the difference between the mean current amplitude was significantly different as a function of channel type. There was no statistical difference in mean current between channel types as a function of external Ca²⁺ concentration. *B*: families of current traces from 2 representative COS-7 cells expressing GIRK1-EGFP + GIRK2 and GIRK2_{wv}-EGFP. Summary of maximum inward current at -160 mV is given to *right* of current traces. Note there was no significant difference in current amplitude in the high external Ca²⁺ solutions between the cells expressing mutant and wild-type channels.

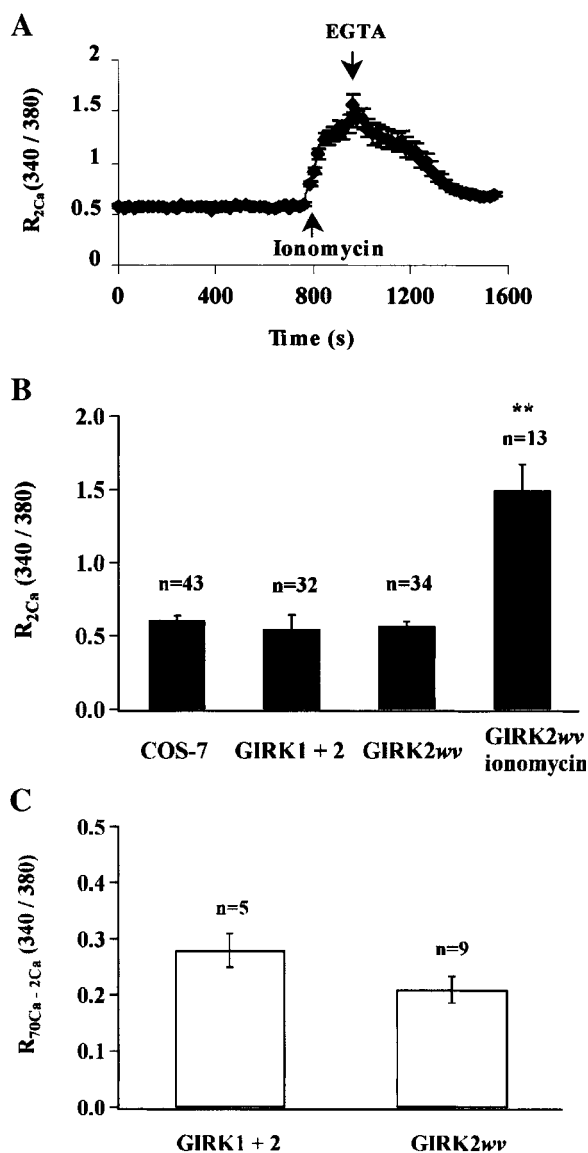


Fig. 7. Comparison of resting Ca^{2+} levels in GIRK1 + GIRK2 vs. GIRK2_{WV}-expressing COS-7 cells. Relative levels of intracellular Ca^{2+} were determined as the 340/380 nm fluorescence intensity ratio ($R_{340/380}$) in fura 2 loaded COS-7 cells expressing either GIRK1 + GIRK2 or GIRK2_{WV} using digital imaging techniques. **A**: resting levels of $R_{340/380}$ in 13 cells before and after exposure to external solutions containing 10 μ M ionomycin. Ionomycin-containing solution was added at arrow. When the $R_{340/380}$ appeared to reach a maximum value, the external solution was changed to one containing 0 mM Ca^{2+} and 1 mM EGTA. **B**: plot of the average resting $R_{340/380}$ in nontransfected cells, cells expressing GIRK1 + GIRK2, and cells expressing GIRK2_{WV} in an external solution containing 2 mM Ca^{2+} . Average maximal response to ionomycin in the GIRK2_{WV} cells is shown in bar at right. **C**: comparison of the difference in resting $R_{340/380}$ for cells in external solutions containing 70 mM Ca^{2+} minus that obtained in 2 mM Ca^{2+} . Cells were exposed to the Ca^{2+} -containing solutions and the differences in the response in the individual cells averaged. There was no significant difference in the response between the GIRK1 + GIRK2 expressing cells over that obtained for the GIRK2_{WV}-expressing cells.

show 1) an elevation of inward current over those expressing the wild-type GIRK1/2 and 2) a shift in reversal potential on switching from low- to high- Ca^{2+} -containing external solutions. These results were ob-

tained in the presence of high concentrations of internal BAPTA to inhibit activation of contaminating Ca^{2+} -activated Cl^{-} currents. Similar experiments in transfected COS-7 cells failed to demonstrate either a significant increase in Ca^{2+} current through the mutant channels over that observed in GIRK1/2-expressing cells or a shift in reversal potential on increases in extracellular Ca^{2+} . We were also unable to observe any significant increase in the resting levels of Ca_i in COS-7 cells expressing GIRK2_{WV} over that observed in non-transfected cells or cells expressing GIRK1/2. Taken together, these data indicate that the divalent cation properties of the expressed GIRK2_{WV} conductance differ between the two heterologous expression systems. Most importantly, however, the data strongly suggest that, if the mammalian cells are a better model for channel expression in mouse neurons than the oocytes, the elevated Ca_i levels observed in *weaver* neurons (4, 21) may be a result of chronic depolarization and not Ca^{2+} influx through the GIRK2_{WV} channels themselves. Evidence in support of this hypothesis comes from the studies of Liesi and Wright (10) who demonstrated that Ca^{2+} channel function is essential in mediating the *weaver* gene effect. The rescue effect of *weaver* granule cell neurons at high but not low concentrations of MK-801 in the studies of Liesi and Wright (10) was consistent with the reported inhibitory effect of verapamil and high concentrations of MK-801 on voltage-gated Ca^{2+} channels; low concentrations of MK-801 (1 μ M) had no rescue effect (10).

Determination of the Ca^{2+} permeability of the homomultimeric GIRK2_{WV} channel is more direct in mammalian cells lacking the contaminating endogenous Ca^{2+} -activated anion conductance. In our experiments, we found no evidence for Ca^{2+} flux through GIRK2_{WV} channels monitored as either an increase in inward current in high divalent solution or in measurements of changes in resting Ca_i as monitored by ratiometric intracellular fura 2 fluorescence. Consistent with the previous anecdotal observation made by Navarro and co-workers (13), we were unable to observe an increase in inward current in Chinese hamster ovary (data not shown) as well as COS cells transfected with the GIRK2_{WV} gene in 70 mM Ca^{2+} containing external solutions.

It is tempting to generalize that the *weaver* mutation in the signature sequence of all K⁺ selective channels would produce a similar loss in K⁺ selectivity in the outwardly as well as the inwardly rectifying K⁺ conductances. Interestingly, this same mutation has been found in a member of the six-transmembrane family of K⁺ channels, which points to the contrary. The K⁺ channel, KCNQ4, localizes its expression to cochlear outer hair cells and maps to the DFNA2 locus for a form of nonsyndromic dominant deafness (7). A mutation in this gene in the DNFA2 pedigree exchanges the G for an S (G285S) in the GYG sequence in the pore of that channel, identical to the mutation in GIRK2_{WV}. The G285S mutation in KCNQ4 exerts a strong dominant negative effect on wild-type KCNQ4, and its loss leads to slow cellular degeneration (7), although the precise

pathogenesis is unknown. KCNQ4 codes for a six-transmembrane domain K⁺ channel subunit protein that is assumed to form a functional heterotetramer with other members of the KCNQ family. Unlike GIRK2_{wv}, which has an equivalent mutation in the signature sequence, the mutation G285S in KCNQ4 does not appear to form functional homomultimers as does GIRK2_{wv}. Coexpression studies with the mutant KCNQ4 G285S and other members of the KCNQ family carried out to date show that coexpression of the mutant subunit reduces current expression by ~90%. The remaining current is K⁺ selective over Na⁺ or Ca²⁺ (7), unlike the selectivity profile of the mutant GIRK2_{wv}. Thus similar pore mutations in the outward and inwardly rectifying K⁺ channel families would appear to have significantly different functional phenotypes with respect to changes in channel selectivity and ability to form functional homo- and heteromultimers (6, 16). The two transmembrane domain GIRK subunits appear to tolerate changes in pore-forming residues allowing for the formation of hetero- as well as homomultimeric channels. The six-transmembrane domain K⁺ channels appear to require a more rigid scaffolding intolerant of similar changes in pore-forming residues.

In addition to the observed differences in selectivity between GIRK1/GIRK2 heteromultimers and GIRK2_{wv} homomultimers, we observed a consistent difference in the kinetics of current activation for the two channels at the most hyperpolarized potentials when expressed in *Xenopus* oocytes. Current activation for GIRK2_{wv} expressed in oocytes was instantaneous, whereas the kinetics of activation for GIRK1/GIRK2 were much slower. Similar differences in the time course of current activation on hyperpolarization between recombinant GIRK1/GIRK2 and GIRK2_{wv} channels have been observed by Slesinger et al. (16). Differences in time course of current activation between the wild-type GIRK1/GIRK2 channels and the mutant GIRK2_{wv} channels were not observed when the recombinant channels were expressed in the mammalian cell background. These differences in activation kinetics, which we observed exclusively in the oocyte expression experiments, are consistent with the weak inward rectification of the currents also observed for the mutant GIRK2_{wv} channel in the oocyte system in our studies as well as those of Kofuji et al. (6). Rectification in the inwardly rectifying K⁺ channels is a result of Mg²⁺ and/or polyamine binding to an intracellular site, thereby blocking monovalent cation permeation in the outward direction (3, 11, 17, 19). It may be that the reduced rectification seen for GIRK2_{wv} when expressed in oocytes may be due to weak binding and/or permeation of a class of cytoplasmic polyamines not present in the mammalian cells.

In summary, results for our investigation indicate that the modest Ca²⁺ influx through GIRK2_{wv} homomeric channels expressed in oocytes differs from that observed for channels expressed in mammalian cells and may represent the formation of a functional channel arising from coassembly with an unidentified endog-

enous subunit of the oocyte. Coassembly with the endogenous *Xenopus* oocyte subunit GIRK5 is unlikely, in that our experiments were conducted using antisense against GIRK5, which would have prevented its expression. Recombinant GIRK2_{wv} channel expression in mammalian cells was not associated with either an observable Ca²⁺ permeation through the conductance nor an increase in intracellular Ca_i over that observed in nontransfected cells. Our data suggest that the elevation in Ca_i associated with neuronal cell death in murine cells expressing the gene may not be due to divalent permeation through the GIRK2_{wv} homomeric channels but may be due instead to toxicity induced through chronic depolarization, allowing for Ca²⁺ influx through voltage-dependent Ca²⁺-permeable pathways.

We thank Drs. Aaron P. Fox, G. Breitwieser, and D. A. Hanck for many helpful discussions as well as Boris Krupa for technical assistance.

This work was supported by National Institute of General Medical Sciences Grants RO1 GM-36823 and RO1 GM-54266.

Address for reprint requests and other correspondence: D. J. Nelson, The Univ. of Chicago, Dept. of Neurobiology, Pharmacology and Physiology, MC0926, 947 East 58th St., Chicago, IL 60637 (E-mail: dnelson@drugs.bsd.uchicago.edu).

Received 30 April 1999; accepted in final form 21 December 1999.

REFERENCES

1. Charnet P, Bourinet E, Dubel SJ, Snutch TP, and Nargeot J. Calcium currents recorded from a neuronal α_{1c} L-type calcium channel in *Xenopus* oocytes. *FEBS Lett* 344: 87–90, 1994.
2. Dascal N, Snutch TP, Lubbert H, Davidson N, and Lester HA. Expression and modulation of voltage-gated calcium channels after RNA injection in *Xenopus* oocytes. *Science* 231: 1147–1150, 1986.
3. Fakler B, Brändle U, Glowatzki E, Weidemann S, Zenner H-P, and Ruppersberg JP. Strong voltage-dependent inward rectification of inward rectifier K⁺ channels is caused by intracellular spermine. *Cell* 80: 149–154, 1995.
4. Fox AP, Dlouhy S, Ghetti B, Hurley JH, Nucifora PGP, Nelson DJ, Won L, and Heller A. Altered responses to potassium in cerebellar neurons from *weaver* heterozygote mice. *Exp Brain Res* 123: 298–306, 1998.
5. Hedin KE, Lim NF, and Clapham DE. Cloning of a *Xenopus laevis* inwardly rectifying K⁺ channel subunit that permits GIRK1 expression of I_{KACH} currents in oocytes. *Neuron* 16: 423–429, 1996.
6. Kofuji P, Hofer M, Millen KJ, Millonig JH, Davidson N, Lester HA, and Hatten ME. Functional analysis of the *weaver* mutant GIRK2 K⁺ channel and rescue of *weaver* granule cells. *Neuron* 16: 941–952, 1996.
7. Kubisch C, Schroeder BC, Friedrich T, Lütjohann B, El-Amraoui A, Marlin S, Petit C, and Jentsch TJ. KCNQ4, a novel potassium channel expressed in sensory outer hair cells, is mutated in dominant deafness. *Cell* 96: 437–446, 1999.
8. Kubo Y, Reuveny E, Slesinger PA, Jan YN, and Jan LY. Primary structure and functional expression of a rat G-protein-coupled muscarinic potassium channel. *Nature* 364: 802–806, 1993.
9. Leonard JP, Nargeot J, Snutch TP, Davidson N, and Lester HA. Ca channels induced in *Xenopus* oocytes by rat brain mRNA. *J Neurosci* 7: 875–881, 1987.
10. Liesi P and Wright JM. Weaver granule neurons are rescued by calcium channel antagonists and antibodies against a neurite outgrowth domain of the B2 chain of laminin. *J Cell Biol* 134: 477–486, 1996.
11. Lopatin AN, Makhina EN, and Nichols CG. Potassium channel block by cytoplasmic polyamines as the mechanism of intrinsic rectification. *Nature* 372: 366–369, 1994.
12. Moorman JR, Zhou Z, Kirsch GE, Lacerda AE, Caffrey JM, Lam DMK, Joho RH, and Brown AM. Expression of single

- calcium channels in *Xenopus* oocytes after injection of mRNA from rat heart. *Am J Physiol Heart Circ Physiol* 253: H985–H991, 1987.
13. **Navarro B, Kennedy ME, Velimirovic B, Bhat D, Peterson AS, and Clapham DE.** Nonselective and G $\beta\gamma$ -insensitive *weaver* K⁺ channels. *Science* 272: 1950–1953, 1996.
 14. **Silverman SK, Kofuji P, Dougherty DA, Davidson N, and Lester HA.** A regenerative link in the ionic fluxes through the *weaver* potassium channel underlies the pathophysiology of the mutation. *Proc Natl Acad Sci USA* 93: 15429–15434, 1996.
 15. **Silverman SK, Lester HA, and Dougherty DA.** Subunit stoichiometry of a heteromultimeric G protein-coupled inward-rectifier K⁺ channel. *J Biol Chem* 271: 30524–30528, 1996.
 16. **Slesinger PA, Patil N, Liao YJ, Jan YN, Jan LY, and Cox DR.** Functional effects of the mouse *weaver* mutation on G protein-gated inwardly rectifying K⁺ channels. *Neuron* 16: 321–331, 1996.
 17. **Tagliatela M, Ficker E, Wible B, and Brown AM.** Pharmacological implications of inward rectifier K⁺ channels regulation by cytoplasmic polyamines. *Pharmacol Res* 32: 335–344, 1995.
 18. **Tucker SJ, Pessia M, Moorhouse AJ, Gribble F, Ashcroft FM, Maylie J, and Adelman JP.** Heteromeric channel formation and Ca²⁺-free media reduce the toxic effect of the *weaver* K_{ir} 3.2 allele. *FEBS Lett* 390: 253–257, 1996.
 19. **Vandenberg CA.** Inward rectification of a potassium channel in cardiac ventricular cells depends on internal magnesium ions. *Proc Natl Acad Sci USA* 84: 2560–2564, 1987.
 20. **White MM and Aylwin M.** Niflumic and flufenamic acids are potent reversible blockers of Ca²⁺-activated Cl⁻ channels in *Xenopus* oocytes. *Mol Pharmacol* 37: 720–724, 1990.
 21. **Womack M, Thompson K, Fanselow E, Augustine GJ, and Peterson A.** Elevated intracellular calcium levels in cerebellar granule neurons of *weaver* mice. *Neuroreport* 9: 3391–3395, 1998.

